

TEMPERATE FOREST HEIGHT ESTIMATION PERFORMANCE USING ICESAT GLAS DATA FROM DIFFERENT OBSERVATION PERIODS

Yong Pang^{a, b, *}, Michael Lefsky^a, Guoqing Sun^c, Mary Ellen Miller^a, Zengyuan Li^b

^a Center for Ecological Applications of Lidar, College of Natural Resources, Colorado State University, Fort Collins, CO 80523, USA

^b Institute of Forest Resource Information Technique, Chinese Academy of Forestry, Beijing 100091, China

^c Department of Geography, University of Maryland, College Park, MD 20742, USA

Commission VII, WG VII/5

KEY WORDS: Temperate Forest Height, Large Footprint Lidar waveform, ICESat GLAS, Observation Period

ABSTRACT:

To investigate the forest height estimation potential and performance of different observation periods GLAS data in temperate region, this study uses the Northeast of China as test site. USFS FIA style field plots were collected. Two methods were used in this study to analyze different period data, i.e., i) the forest height analysis for those waveforms who have field measurements, ii) the near repeat observations analysis for those waveforms whose waveform center location is within 10 meters. The results show that the summer period GLAS waveforms capture the returns from forest canopy. The data from early stage of autumn period still contain enough returns from forest canopy, even with lower intensity. The spring period and late autumn period data contain less signals from forest canopy and difficult to estimate forest height. Further analysis will be carried out for all temperate forest areas and use appropriate periods data to generate forest height map for temperate forests.

1. INTRODUCTION

Laser altimeter systems provide high-resolution, geolocated measurements of vegetation vertical structure and ground elevations beneath dense canopies. The basis of this method is ranging to a surface obtained by precise timing of the round-trip travel time of short-duration pulses of near-infrared laser radiation (Lefsky et al., 2002). The Geoscience Laser Altimeter System (GLAS) aboard the Ice, Cloud and land Elevation Satellite (ICESat) is a waveform sampling lidar sensor. It records the power of energy reflected from the ground surface as a function of time. When that surface is vegetated, the return echoes, or waveforms, are a function of the vertical distribution of vegetation and ground surfaces within the area illuminated by the laser (the footprint). The GLAS has acquired over 250 million individual lidar observations over forest regions globally, each of which can be used to derive topographic and vegetation height information. Some studies have shown accurate vegetation heights can be retrieved from these measurements (Harding and Carabajal, 2005; Lefsky et al., 2005 and 2007; Sun et al., 2008).

These data provide an unprecedented global vegetation height dataset. The main objective of the ICESat mission is to measure ice sheet elevations and changes in elevation through time. Secondary objectives include measurement of cloud and aerosol height profiles, land elevation and vegetation cover, and sea ice thickness. After its first laser break, GLAS operates its two remaining lasers for three 33-day campaigns per year to maximize its duration and meet its main objective. The spring period is from February to March, the summer period is from May to June and the autumn period is from October to November. These three periods correspond to different phenological status of temperate forests. As the LiDAR

waveform is a function of the vertical distribution of vegetation and ground surfaces within the area illuminated by the laser (the footprint), the variances of the mass of tree leaves and leaf optical characteristics will change the intensity and shape of LiDAR waveforms and take effects on the estimated forest parameters.

Sun et al. (2008) compared GLAS waveforms from October and June and attributed the waveform width differences to different densities of foliage. Duong et al. (2008) analyzed winter and summer (2003) along near coincident ground tracks. The Height of Median Energy (HOME) changed most in broad-leaved (a 148% change) and least for conifers (a 36% change, winter to summer).

To investigate the forest height estimation potential and performance of different observation periods GLAS data in temperate region, this study uses the Northeast of China as test site. Both the field data and near repeat footprints from different observation periods were used.

2. STUDY AREA AND FIELD DATA

The study area is the Northeast of China, which includes the Heilongjiang province, Jilin Province, Liaoning Province and the eastern Inner Mongolia. Forests are mainly distributed on the mountains. This region has abundant tree species and a variety of forest types, including evergreen needleleaf forest, deciduous needleleaf forest, deciduous broadleaf forest, and mixed forests. The dominant species are larch (*Larix gmelinii*), birch (*Betula platyphylla*), pine (*Pinus sylvestris var. mongolica*) and oak (*Quercus mongolica*). Most forests are deciduous. The

* Corresponding author: caf.pang@gmail.com

evergreen needleleaf forests only distribute in small part of Changbaishan, Xiaoxinganling and Daxinganling.

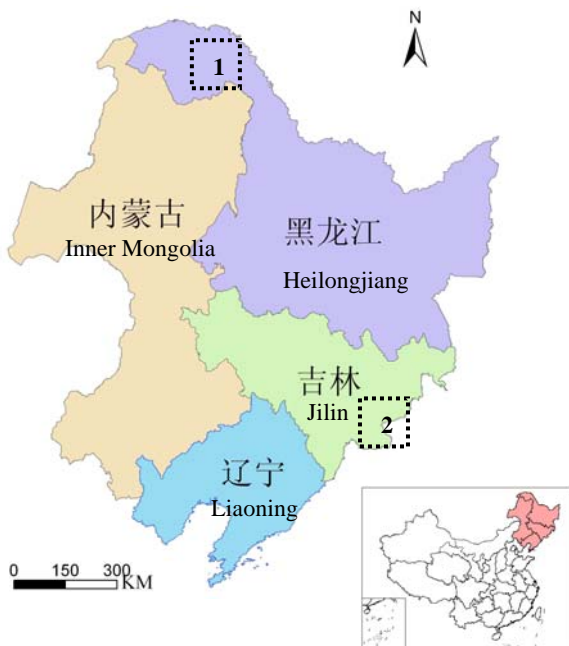


Figure 1 Location of Northeast China

Two test sites have been selected, which are located in the Daxinganling (square 1 in Figure 1) and Changbaishan (square 2 in Figure 1) forest regions. Intensive field works has been conducted. 82 GLAS footprints were measured in these two sites. USFS FIA style field plots were measured. After the center of GLAS footprint was located using DGPS, four sampling plots with a radius of 7.5 m (center plot, and three satellite plots which are 22.5 m to 0°, 120°, and 240° bearing direction relative to the center plot) were located within the footprint. Within each plot area, diameter at breast height (dbh, where breast height = 1.37 m) and height of all trees with DBH greater than or equal to 5 cm were measured and recorded. Tall and dominant trees within a 50 m radius circle centered by GLAS footprint but not inside these 4 sampling plots were also measured. These measurements were used to estimate the Lorey's height for each footprint.

3. REMOTE SENSING DATA

3.1 ICESat GLAS data

Data from several GLAS observation periods between 2003 and 2006 were used. During this period, eleven observation periods of GLAS data were collected. For this research, GLAS data from the ICESat Vegetation Product (IVP- Lefsky, In Prep) were used. The IVP combines vegetation relevant information from GLAS records GLA01, GLA05, GLA06 and GLA14.

GLAS records the returned laser energy from an ellipsoidal footprint. The nominal footprint diameter is about 70 m in diameter, but its size and ellipticity have varied through the course of mission. The computed sizes determined from instrumentation on board the spacecraft are closer to about 110,

90 and 55 m for lasers 1, 2, and 3 respectively (http://nsidc.org/data/icesat/glas_laser_ops_attrib.pdf).

To estimate forest canopy height from GLAS waveforms (stored in GLA01 product), several waveform indices were calculated. Waveform extent is defined as the vertical distance between the first and last elevations at which the waveform energy exceeds a threshold level. In this work, the threshold was determined using ICESat data product estimates of the mean and standard deviation of background noise (ICESat product variables D_4NSBGMEAN and D_4NSBGSDDEV). Removal of the effects of terrain slope and canopy height variability relies on two indices of waveform structure. The trailing edge extent is calculated from the waveform as the absolute difference between the elevation of the signal end and the elevation at which the signal strength of the trailing edge is half of the maximum signal above the background noise value. Similarly, the leading edge extent is determined as the absolute difference between the elevation of the signal start and the elevation at which the signal strength of the leading edge is half of the maximum signal above the background noise value. At the leading edge of the waveform, the "signal start" threshold crossing indicates the elevation of the uppermost foliage and/or branches that were detected, and the trailing edge threshold crossing indicates the elevation of the lowest illuminated surface, or the "signal end". Where sufficient laser energy is reflected from the ground, "signal end" crossing represents the lowest detected ground surface. Details of GLAS processing and ICESat GLAS Vegetation Product (IVP) produces can be found in Lefsky et al. (2007 and In Prep).

3.2 NDVI Dataset

NDVI from the NOAA AVHRR Global Vegetation Index product for the associated 8 day period were used to justify where are forests and the vegetation vigour status when GLAS pulse fired.

3.3 SRTM DEM Dataset

The 90 m the Shuttle Radar Topography Mission (SRTM) product were used as DEM information for each GLAS shot (<http://www.jpl.nasa.gov/srtm>). The dual antenna system of SRTM provides the best elevation data ever available at a global scale. Slope and elevation range were extracted from 3 by 3 window centered by GLAS footprint. For vegetated areas, SRTM DEMs represent the radar phase center elevation, which depends on canopy structure and fractional cover, and are an approximation for ground elevation.

4. METHODS

4.1 Estimation Forest Height from Different Observation Period GLAS Data

Generally, forest height is estimated from the waveform start to ground peak. But with the slope of the terrain and/or the size of the footprint increases, a greater range of terrain elevations are sampled and the ability to directly relate forest height to the waveform decreases (Pang and Lefsky, 2008). Because vegetation characteristics and terrain slope interact, it is difficult to develop an analytical equation to describe this effect. Lefsky et al. (2005) used ancillary topography information from SRTM to correct for slope effects and estimate maximum forest height in three ecosystems: tropical broadleaf forests in Brazil,

temperate broadleaf forests in Tennessee, and temperate needle leaf forests in Oregon (Lefsky, et al., 2005). Rosette et al (2008) verified this method in England. Lefsky et al. (2007) developed an approach for slope correction based only on the information in the GLAS waveform itself. This method was used to estimate forest height in this research, i.e., use the waveform extent, trailing edge and leading edge from GLAS waveform directly. The basal area weighted mean height (Lorey's height) was calculated for each field plots.

4.2 Extraction of Overlapping Waveform Pairs from IVP Product

Delaunay triangulation was used to find all the possible nearest neighbor shots. Since Delaunay triangulations have the property that the circum-circle of any triangle in the triangulation contains no other vertices in its interior, the possible nearest neighbor shots are only computed from nearby points. Then a distance threshold was used to justify whether two GLAS shots constructed an overlap pair. Considering the GLAS footprint size (radius varies from 28 to 55 m), 10 m distance threshold was used to ensure the overlapping pair contains certain common part. To compare the seasonal effects of GLAS observation, only waveforms pairs from different observation campaigns are considered.

4.3 Extract NDVI and DEM Information for Overlapping Waveform Pairs

According to previous studies, the height estimation difference for evergreen forests is very small from different observation periods GLAS data (Duong et al. 2008; Pang et al., 2008). And there were some differences for deciduous forests (Sun et al., 2008; Duong et al. 2008). The NDVI was used to justify where are forests and the vegetation vigour status where GLAS pulse fired. The NDVI_max above 160 were assumed as coming from forests.

To avoid the terrain slope and heterogeneous effects, the slope of those pairs less than 10 degree were used.

4.4 Overlapping Waveform Pairs Analysis

Generally, barren land, cropland and grassland have small waveform extent and show good consistent seasonally. To avoid too many samples from these non-forest types, all the records with waveform extent less than 5 m were removed. To eliminate those waveforms reflected from clouds, any record with maximum waveform intensity in a pair low than 80 was removed from further analysis.

Then the overlapping dataset were compared by different period. The waveform extent, trailing edge and leading edge were compared. The linear regression like eq. 1 was used to compare these waveform variables among different periods.

$$y = ax + b \tag{1}$$

where: a is slope and b is constant.

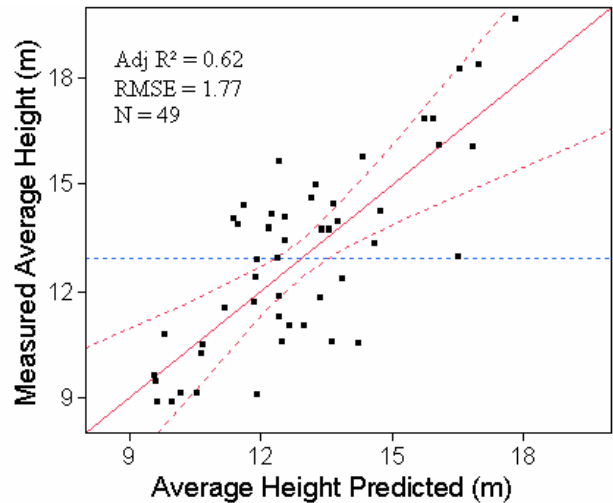
The correlate coefficient and RMSE were calculated for each combination.

5. RESULTS AND DISCUSSION

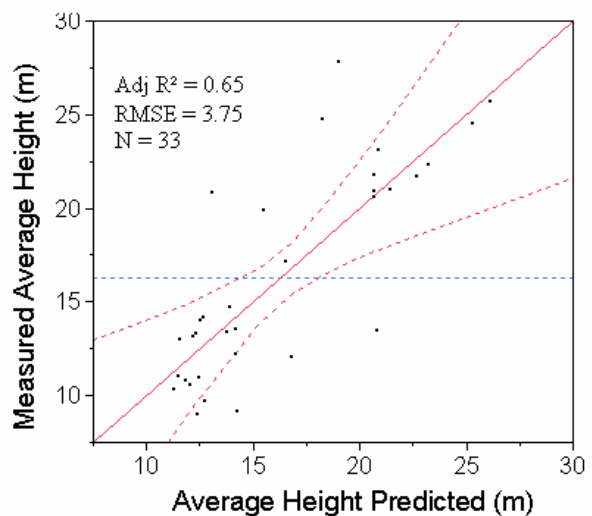
5.1 Estimation Forest Height from Different Observation Period GLAS Data using Field Measurements

Figure 2 shows a comparison of average tree height from field measurements and the estimation from waveforms using all 82 field plots. Figure 2(a) shows the results from summer season GLAS observations, i.e., L3C and L3F. Figure 2(b) shows the results from autumn season GLAS observations, i.e., L2A, L3A, L3D and L3G.

The correlation coefficients of these two season combinations are pretty high. The RMSE of the summer season (1.77 m) is much less than that of autumn season (3.75 m). And the regression coefficients of different waveform variables are different for these two cases, which shows different correction quantity should be used for the temperate forest height estimation. The 1064 nm reflectance decreases in autumn, which would change waveform shape, then the waveform variables, especially leading edge.



(a) L3C and L3F



(b) L2A, L3A, L3D and L3G

Figure 2. Estimation forest height from different observation period GLAS data using field measurements

5.2 Waveform Matrices Analysis using Overlapping Waveform Dataset

Figure 3 compares two waveforms from a very dense deciduous forest in April and June. It is obvious that the waveform from June has much stronger canopy returns, even the ground returns are similar. For the spring waveform, the crown return is so weak that it tends to underestimate waveform extent and overestimate leading edge. On the other hand, it is easier to detect waveform extent from the summer waveform. But the ground return is weaker relative to the canopy return, which tend to overestimate trailing edge.

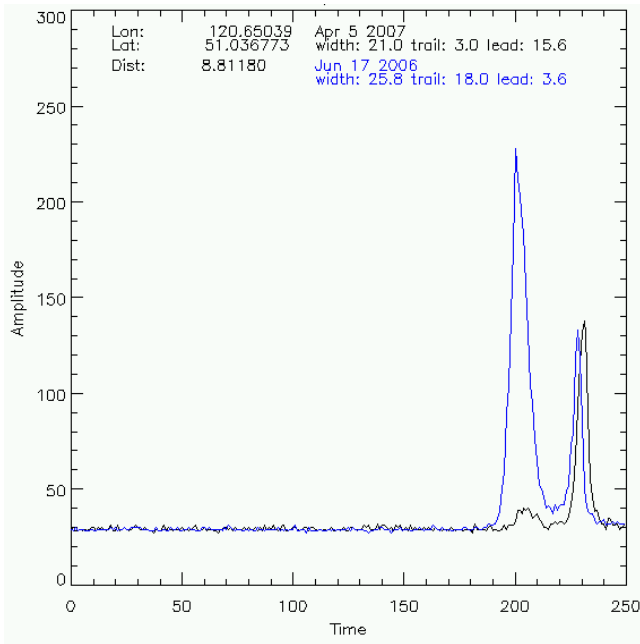


Figure 3. Comparison of GLAS waveforms from different observation periods (the unit of x axis is 4 ns)

Table 1 shows the linear regression results for all the combinations from L2A to L3G. For each waveform variable (i.e., waveform extent, trailing edge and leading edge), correlation coefficient, RMSE, slope and constant were estimated.

For waveform extent, most same season combinations shows good consistence. The summer-summer combination (L3CL3F) demonstrated lowest RMSE (2.96) and very high correlation coefficient (0.85). But the inter-laser also takes large effects on the relationship, for example, L2AL3D has largest RMSE (12.36). This might caused by the large footprint size and orientation differences between Laser2 and Laser3.

Most summer-spring/autumn combinations show large RMSE (> 6) and low correlation coefficient (<0.6). Some of the spring-autumn combinations showed good consistent. In such combinations, most of autumn data is from November, which deciduous shows similar phenology with early spring season. The trailing edge and leading edge showed similar patterns with waveform extent.

6. CONCLUSION AND FUTURE WORK

The results show that the summer period GLAS waveforms capture the returns from forest canopy. The data from early stage of autumn period still contain enough returns from forest

canopy, even with lower intensity. The forest height estimation equation may parameterize separately for different season GLAS data. The spring period and late autumn period data contain less signals from forest canopy and difficult to estimate forest height. Further analysis will be carried out for all temperate forest areas and use appropriate periods data to generate forest height map for temperate forests.

Further study is required regarding precise forest classification map and forest disturbances information from other dataset to eliminate effects of evergreen forests, forest disturbance, such as logging, fire, disease and insect.

ACKNOWLEDGMENT

The authors would like to thank the help on the field measurement: Dr. Guo Z., Liu D., Wang D., Fu A., Wang X., Ni W. for attending some field measurement; the Forest Bureau of Tahe, Lushuihe, and Changbai Forest Ecology Research Station for providing local lodging, transportation and help to access these forest plots. This study was funded by National Science Foundation of China (40601070), the 863 program (2007AA12Z173) and NASA cryosphere program "A Global Forest Canopy Height and Vertical Structure Product from the Geoscience Laser Altimeter System".

REFERENCES

- Duong; V. H., R. Lindenbergh, N. Pfeifer, & G. Vosselman. (2008). Single and two epoch analysis of ICESat full waveform data over forested areas. *International Journal of Remote Sensing*, 29(5), 1453-1473
- Harding, D.J., and Carabajal, C.C. (2005). ICESat waveform measurements of within-footprint topographic relief and vegetation vertical structure. *Geophysical Research Letters*, 32: L21S10, doi:10.1029/2005GL023471.
- Lefsky, M.A., Cohen, W.B., Parker, G.G., & Harding, D.J. (2002). LiDAR remote sensing for ecosystem studies. *Bioscience*, 52(1), 19-30.
- Lefsky, M. A., Harding, D. J., Keller, M., Cohen, W. B., Carabajal, C. C., Espirito-Santo, F. D., et al. (2005). Estimates of forest canopy height and aboveground biomass using ICESat. *Geophysical Research Letters*, 32, L22S02.
- Lefsky, M. A., Harding, D., Cohen, W. B., Parker, G., & Shugart, H.H. (1999). Surface lidar remote sensing of basal area and biomass in deciduous forests of Eastern Maryland, USA. *Remote Sensing of Environment*, 67, 83-98.
- Lefsky, M.A., Keller, M., Pang, Y., de Camargo, P., & Hunter M.O. (2007). Revised method for forest canopy height estimation from the Geoscience Laser Altimeter System waveforms. *Journal of Applied Remote Sensing*, 1, 013537
- Lefsky, M.A. et al. In Prep. A Global Forest Canopy Height Dataset from the Geoscience Laser Altimeter System.
- Pang, Y., and Lefsky, M. (2008) (Submitted). Terrain Effects Simulation and Model based Height Correction for Large Footprint LiDAR Waveforms from Coniferous Forests.
- Pang, Y., Lefsky, M., Andersen, H., Miller M. E., and Sherrill K. (2008) (Submitted). Automatic Tree Crown Delineation using Discrete Return LiDAR Data and its Application in ICESat Vegetation Product Validation
- Rosette, J., North, P. & Suárez, J. (2008). Vegetation Height Estimates for a Mixed Temperate Forest using Satellite Laser Altimetry. *International Journal of Remote Sensing*, 29(5), 1475-1493

Sun, G., Ranson, K.J., Kimes, D.S., Blair, J.B., & Kovacs, K. (2008). Forest vertical structure from GLAS: An evaluation using LVIS and SRTM data. *Remote Sensing of Environment*, 112(1), 107-117.

periods	Waveform extent (WE)				Trailing edge (T)				Leading edge (L)			
	r ² _WE	rmse_WE	a_WE	b_WE	r ² _T	rmse_T	a_T	b_T	r ² _L	rmse_L	a_L	b_L
L2AL2B	0.854	6.68	0.864	3.121	0.864	2.558	0.807	0.915	0.711	5.196	0.678	2.808
L2AL3A	0.811	7.288	0.735	3.64	0.751	4.086	0.602	1.722	0.658	4.315	0.489	2.392
L2AL3B	0.775	7.919	0.719	6.275	0.554	3.166	0.477	2.468	0.743	4.71	0.709	2.731
L2AL3C	0.726	6.602	0.493	6.683	0.713	2.872	0.324	1.97	0.549	3.927	0.366	3.068
L2AL3D	0.747	12.359	1.18	3.251	0.725	6.5	1.139	2.333	0.534	6.493	0.572	5.2
L2AL3E	0.722	6.825	0.667	5.678	0.727	3.151	0.552	1.746	0.684	3.82	0.656	2.308
L2AL3F	0.737	7.452	0.699	6.551	0.682	3.734	0.582	2.589	0.248	5.651	0.254	6.397
L2AL3G	0.845	6.164	0.881	1.285	0.787	3.441	0.683	1.297	0.642	4.727	0.717	1.248
L2BL2C	0.336	5.526	0.457	6.019	0.077	1.952	0.209	1.166	0.361	3.797	0.493	1.892
L2BL3A	0.774	6.125	0.771	4.81	0.732	2.836	0.647	1.862	0.589	4.42	0.584	3.589
L2BL3B	0.874	4.427	0.926	1.334	0.711	2.877	0.729	1.171	0.865	3.084	0.866	0.911
L2BL3C	0.778	4.96	0.624	5.622	0.584	2.318	0.299	2.59	0.75	3.067	0.682	1.457
L2BL3D	0.881	6.443	0.891	-0.251	0.788	3.158	0.612	0.88	0.797	3.854	0.756	0.404
L2BL3E	0.621	8.166	0.583	6.899	0.54	3.866	0.323	3.352	0.543	4.818	0.571	2.556
L2BL3F	0.722	8.325	0.754	7.589	0.583	4.869	0.486	3.477	0.266	6.782	0.154	7.454
L2BL3G	0.649	7.871	0.571	8.094	0.498	3.723	0.337	3.348	0.706	4.261	0.7	2.291
L2CL3A	0.128	6.317	-0.033	11.865	-0.253	2.795	-0.231	2.886	0.311	3.93	0.12	2.894
L2CL3B	0.643	3.404	0.675	3.119	0.491	1.254	0.497	0.703	0.511	2.408	0.7	0.742
L2CL3C	0.615	5.984	0.616	5.168	0.459	2.248	0.413	1.273	0.52	3.976	0.417	2.469
L2CL3D	0.83	4.376	0.803	2.559	0.722	2.503	0.692	0.836	0.713	3.883	0.596	2.092
L2CL3E	0.787	6.092	0.786	3.602	0.737	2.678	0.747	1.347	0.498	5.076	0.457	3.64
L2CL3F	0.675	6.37	0.445	5.021	0.116	1.841	0.032	1.282	0.614	4.55	0.473	1.047
L2CL3G	0.847	8.364	1.156	-1.323	0.762	4.573	0.608	2.143	0.462	4.708	0.416	3.415
L3AL3B	0.916	4.367	0.926	1.723	0.868	2.292	0.831	1.037	0.838	3.023	0.841	1.354
L3AL3C	0.586	7.463	0.544	14.127	0.678	3.056	0.541	2.744	0.198	5.975	0.202	7.792
L3AL3D	0.877	5.442	0.894	2.501	0.78	2.341	0.79	1.013	0.823	4.479	0.811	1.654
L3AL3E	0.843	5.062	0.869	2.561	0.794	2.51	0.713	1.368	0.733	3.672	0.745	1.601
L3AL3F	0.799	5.876	0.81	5.237	0.569	5.86	0.626	4.798	0.343	5.22	0.198	5.696
L3AL3G	0.847	4.424	0.837	1.729	0.827	1.786	0.743	0.684	0.757	3.382	0.769	0.741
L3BL3C	0.627	5.246	0.841	1.935	0.639	1.899	0.919	0.516	0.612	3.415	0.557	0.775
L3BL3D	0.793	7.647	0.816	4.921	0.734	3.133	0.697	1.808	0.655	5.532	0.638	3.681
L3BL3E	0.862	5.806	0.855	3.093	0.843	3.079	0.815	1.138	0.692	4.444	0.677	2.32
L3BL3F	0.645	6.388	0.946	0.421	0.7	3.595	0.801	0.913	0.309	6.77	0.239	3.835
L3BL3G	0.931	5.755	0.946	1.113	0.863	4.15	0.778	1.317	0.842	3.861	0.744	1.214
L3CL3D	0.744	6.828	0.749	3.989	0.647	2.973	0.394	2.073	0.591	5.268	0.491	3.077
L3CL3E	0.747	7.192	0.776	3.915	0.733	2.875	0.664	1.315	0.595	5.2	0.54	2.683
L3CL3F	0.851	2.962	0.802	2.103	0.802	0.931	0.81	0.321	0.753	2.594	0.761	0.902
L3CL3G	0.307	8.051	0.364	11.655	0.575	3.183	0.494	2.216	0.21	4.901	0.125	4.588
L3DL3E	0.875	3.659	0.896	1.313	0.843	1.71	0.82	0.486	0.829	2.933	0.827	0.703
L3DL3F	0.361	8.252	0.416	13.017	0.014	4.785	-0.038	5.682	0.126	6.098	0.1	6.742
L3DL3G	0.923	4.784	0.937	1.42	0.835	3.157	0.746	1.306	0.822	3.652	0.756	1.371
L3EL3F	0.576	7.107	0.7	6.994	0.618	2.6	0.663	1.849	0.464	4.331	0.341	3.216

L3EL3G	0.841	5.343	0.851	2.622	0.775	2.644	0.671	1.241	0.751	4.221	0.716	1.885
L3FL3G	0.645	8.422	0.715	6.287	0.655	4.28	0.748	2.296	0.406	5.232	0.21	4.101

Table 1. The linear regression results for all the combinations from L2A to L3G in the Northeast of China